

Dose distribution calculation for *in-vivo* X-ray fluorescence scanning

R.G. Figueroa^a, E. Lozano^b, and M. Valente^{c,d}

^aDepartamento de Ciencias Físicas, Universidad of La Frontera,
Av. Francisco Salazar 01145, Temuco, 4811230, Chile.

^bInstituto Nacional del Cáncer, Unidad de Física Médica,
Av. Profesor Zañartu 1010, Santiago, Chile,

^cCONICET, Buenos Aires, Argentina.

^dUniversidad Nacional de Córdoba, Argentina.

e-mail: figueror@ufro.cl

Received 26 July 2012; accepted 27 February 2013

In-vivo X-ray fluorescence constitutes a useful and accurate technique, worldwide established for constituent elementary distribution assessment. Actually, concentration distributions of arbitrary user-selected elements can be achieved along sample surface with the aim of identifying and simultaneously quantifying every constituent element. The method is based on the use of a collimated X-ray beam reaching the sample. However, one common drawback for considering the application of this technique for routine clinical examinations was the lack of information about associated dose delivery. This work presents a complete study of the dose distribution resulting from an *in-vivo* X-ray fluorescence scanning for quantifying biohazard materials on human hands. Absorbed dose has been estimated by means of dosimetric models specifically developed to this aim. In addition, complete dose distributions have been obtained by means of full radiation transport calculations in based on stochastic Monte Carlo techniques. A dedicated subroutine has been developed using the PENELOPE 2008 main code also integrated with dedicated programs -MatLab supported- for 3D dose distribution visualization. The obtained results show very good agreement between approximate analytical models and full descriptions by means of Monte Carlo simulations.

Keywords: Dosimetry; *in-vivo* X-ray fluorescence; scanning image XRF and Monte Carlo simulation.

La Fluorescencia de rayos-X *in-vivo* constituye una técnica útil y precisa, establecida ampliamente para la evaluación de constituyente de distribución primaria. De hecho las distribuciones de concentración de un elemento seleccionado arbitrariamente por el usuario se pueden lograr a lo largo de la superficie de la muestra con el objetivo de identificar y cuantificar simultáneamente cada elemento constituyente. El método se basa en el uso de un haz colimado de rayos X que incide en la muestra. Sin embargo, un inconveniente común para considerar la aplicación de esta técnica para exámenes clínicos de rutina es la falta de información sobre la administración de la dosis correspondiente. Este trabajo presenta un estudio completo de la distribución de la dosis resultante de un barrido *in-vivo* de Fluorescencia de rayos X para la cuantificación de los materiales biológicos peligrosos en manos humanas. La dosis absorbida se ha estimado por medio de modelos dosimétricos específicamente desarrollados para este fin. Además, las distribuciones de dosis completas se han obtenido por medio de cálculos de transporte de radiación completo en base a técnicas estocásticas de Monte Carlo. Una subrutina dedicada ha sido desarrollada utilizando el código principal PENELOPE 2008 también integrada con programas dedicados de soporte MatLab para la visualización 3D de la distribución de dosis. Los resultados obtenidos muestran una buena concordancia entre los modelos analíticos aproximados y en todas las descripciones por medio de simulaciones de Monte Carlo.

Descriptor: Dosimetría; XRF en vivo; imágenes EDXRF por barrido y simulación Monte Carlo.

PACS: 87.53.Bn; 78.70.En; 87.59.-e

1. Introduction

Nowadays, X-ray fluorescence spectrometry is worldwide employed for many research and applications purposes. This method allows determining elemental composition in different material samples, including solids, liquids and gases. The method is mainly based on the sample irradiation with soft X-ray photons and further detection of the resulting characteristic fluorescent yield.

X-ray fluorescence techniques are mainly used for the study and characterization of inorganic samples, such geological, metallurgic, synthetic oils, paint and so on [1,2]. In addition, the X-ray methods have been also utilized for medical and biological applications, like the well known absorption contrast X-ray radiography [3], mammography [4] and computed tomography [5].

In-vivo X-ray fluorescence scanning is a novel and almost recent technique proposed to assess a suitable way of determining the presence of possible contaminant agents in biological samples and patients [6-8]. In addition, due to the fact that this method is able to perform chemical element spatial distributions, one can also take advantage from it in order to characterize patient bone quality by means of quantifying the bone mineral composition.

Actually, the spatial distribution and concentration of chemical elements in different organs and bone may be an indicator of certain diseases or be out of the tolerable levels. Therefore, the knowledge of the concentration of elements and their spatial distribution can provide important information regarding the health of an individual. In fact, it has been evidenced that high levels of copper are directly correlated with cancer. Particularly, elevated copper levels have been

found in malignant cells in concentrations ranging from 1.5 to 3 times higher when compared to normal values [9]. Similarly, increased levels of Pb can cause different well known diseases in human health, like lead poisoning (saturnism) and high strontium concentrations interfere with the mechanism of calcification of bone matrix, among other effects. High iron levels in blood serum can produce thalassemia and mercury, being a toxic and nonessential element for humans, can cause poisoning by concentration. On the other hand, zinc, calcium and phosphorus, which are vital minerals for humans, are necessary for bone mineralization and particularly helpful for avoiding osteoporosis [10].

However, one the major drawbacks of the *in-vivo* X-ray fluorescence scanning is the delivered dose to patient during the scanning. Therefore, in order to support its implementation, it becomes necessary to perform preliminary dosimetric studies aimed to establish potential risks. It can be found in literature that different authors have published significant different dose levels corresponding to *in-vivo* X-ray fluorescence scanning.

Therefore, this work is devoted to a detailed dosimetric characterization and associated features when biological samples are irradiated with a typical *in-vivo* X-ray fluorescence scanning device. A complete dosimetric study has been performed considering analytical models based on suitably approximations, like pencil beam along with full radiation transport calculation by means of Monte Carlo techniques. The obtained results, which are in good agreement with data in literature, suggest that the *in-vivo* X-ray fluorescence scanning may constitute a non extremely dangerous procedure and therefore it may be considered, when pondering profits and risks, as a reliable and feasible method for detecting and quantifying contaminant elements concentration and distribution.

2. Materials and methods

First at all, dose distribution for *in-vivo* X-ray fluorescence scanning has been calculated by means of different methods: analytical models and Monte Carlo simulations. Then, the performance of the developed *in-vivo* X-ray fluorescence scanning device has been preliminary characterized by means of irradiating a human skeleton phantom.

2.1. Analytical dose calculation

The first attempt has been to develop a simple analytical dosimetric model. Due to the intrinsic characteristics of the *in-vivo* X-ray fluorescence scanning device, which employs high collimated beams, it was natural to propose a method is based on pencil beam algorithms [11,12].

The analytical calculation method required some approximations, narrow beams have been considered as incident radiation, pure energy deposition by means of incident fluence attenuation and originally homogeneous samples, but also heterogeneous media can be modeled.

The method was mainly based on the Lambert-Beer equation, which describes radiation absorption/ transmission across a uniform thickness sample, as indicated below:

$$N(x) = N_0 [1 - e^{-\mu x}] \tag{1}$$

where $N(x)$ indicates the number of photons at depth x , N_0 is the total incident photon number and represents the mass absorption coefficient.

Then, the absorbed dose at depth x , ($D(x)$) has been calculated as the ratio of the delivered energy (dE) to the corresponding volume mass (dm), which need to be weighted according incident radiation fluence:

$$D(x) = \frac{dE}{dm} = \int_0^{E_{max}} E \left(\frac{d^2N}{dm dE} \right) dE \quad [Gy] \tag{2}$$

or equivalently:

$$D(x) = \int_0^{E_{max}} N_0(e) E \left(\frac{d^2(1 - e^{-\mu(E)x})}{\rho A dx dE} \right) dE \quad [Gy] \tag{3}$$

Therefore, introducing radiation source characteristics along with sample properties in Eq. 3 it becomes straightforward to assess the corresponding absorbed dose estimation.

2.2. Absorbed dose by means of Monte Carlo Simulations

The absorbed dose corresponding to the *in-vivo* X-ray fluorescence scanning device has been suitably modeled by means of Monte Carlo simulations. A dedicated subroutine has been adapted in based of the PENELOPE v. 2008 package [13]. The PENELOPE main code has been largely utilized for general purposes radiation transport as well as dosimetric applications [14-17].

The developed code allows introducing the geometry and material composition of the *in-vivo* X-ray fluorescence scanning device along with the sample and radiation source characteristics. The X-ray beam properties have been carefully measured and then introduced to the simulation code in order to keep the best correlation between experimental and virtual models by means of considering the same incident spectrum kernel. Several tallies have been incorporated to the simulation code in order to compute absorbed dose distribution within the irradiated sample by means of a suitable voxelization. Absorbed dose at each voxel position $D(x; y; z)$ was calculated from absorbed energy according to:

$$D(x, y, z) = \frac{1}{m(x, y, z)} \times \left[\sum_i E_i(x, y, z) - \sum_j E_j(x, y, z) \right] \tag{4}$$

where $E_i(x; y; z)$ indicates the energy deposited in the $(x; y; z)$ voxel by i -incoming particles; whereas $E_j(x; y; z)$

indicates the energy carried out by the created secondary particles that leave the $(x; y; z)$ voxel, the index j indicating all secondary particles leaving the $(x; y; z)$ voxel having mass equal to $m(x; y; z)$.

3. Results and discussion

Depth dose distributions within homogeneous and heterogeneous typical biological samples have been calculated by means of the proposed analytical model of Eq. 3 and the obtained results are reported in the Fig. 1.

As shown in the above (Fig. 1), in the homogeneous sample can be seen that as depth increases the dose falls in a continuous exponential, with a maximum at the entrance surface, in contrast to the dose present heterogeneous sample jumps as changes in material reaching maximum value equal to 0.13 mGy/s when radiation enters the bone and the corresponding average value equals to 0.02 mGy/s along the beam path inside the finger.

Similarly, once the *in-vivo* X-ray fluorescence scanning irradiation setup was already introduced to the simulation code, it was possible to achieve absorbed dose values for each body constituting the irradiated sample. In addition, 3D dose distributions have been also assessed by means of the incorporated voxelization subroutine. The obtained results for the depth dose distributions by means of Monte Carlo technique are presented in Fig. 2.

In view of the obtained results reported in Figs. 1 and 2, it should be emphasized that the skin would be the more affected organ whenever *in-vivo* X-ray fluorescence scanning device may apply to routine examinations. In addition, depth dose distributions obtained from analytical model and Monte Carlo technique show similar global trend and an overall good agreement, but in order to highlight quantitative differences, Fig. 3 reports the corresponding in-depth absorbed dose differences for both homogeneous and inhomogeneous media.

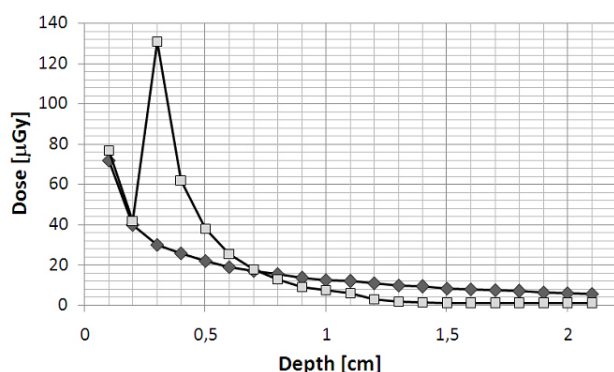


FIGURE 1. Depth dose distribution for homogeneous (diamond) and inhomogeneous (squares) sample obtained with the proposed analytical model.

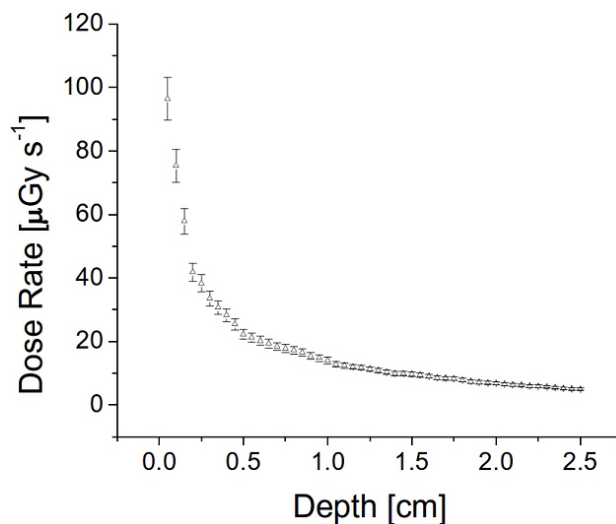


FIGURE 2. Monte Carlo results for the in-depth dose rate for homogeneous (tissue-equivalent) phantom irradiated with the *in-vivo* X-ray fluorescence scanning device.

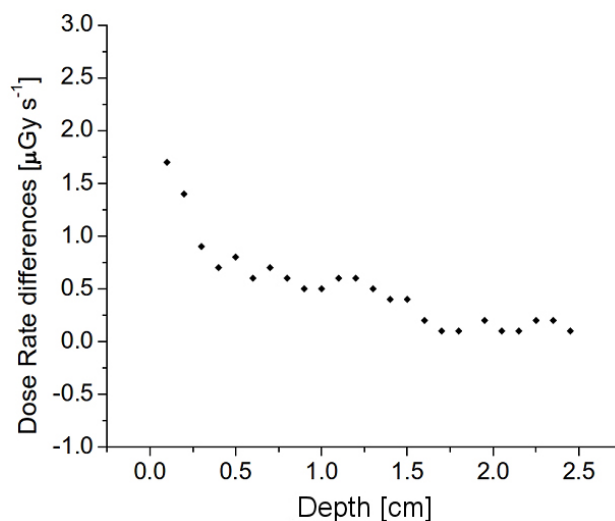


FIGURE 3. Absolute value for in-depth dose rate differences between analytical model and Monte Carlo simulations.

As reported in Fig. 3 both results are coincident and these values are within the ranges of absorbed dose commonly used by conventional *in-vivo* XRF techniques [9].

Therefore, once preliminary dosimetric evaluations and characterization were already accomplished, it became possible to proceed with the study and technical characterization of the developed *in-vivo* X-ray fluorescence scanning device.

After system calibration and optimization, different images have been acquired with the aim of testing the device feasibility. Typical results are reported in Figs. 4 and 5.

The above figures are examples confirming the fact that the technique allows imaging different chemical elements within biological samples, like human and animal bone by means of an average dose rate 0.48 mG/s. Particularly, regarding the jaw shown in Fig. 4, it can be clearly appreciated the achieved good definition of the elements present in the bone.

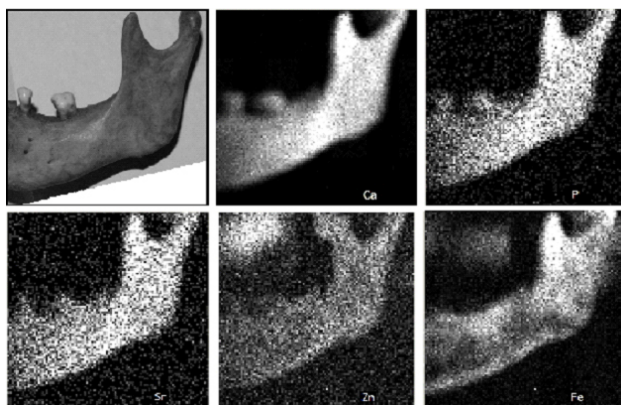


FIGURE 4. Image of the mandible (optical) analyzed together with the corresponding XRF images of the elements Ca, P, Sr, Zn and Fe detected in the jaw. Note the absence of iron teeth.

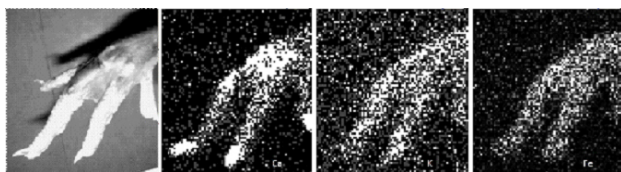


FIGURE 5. Image (optics) a crow's foot (chicken dressing) in the detected Cl, K, Ca, Ti, Fe, Cu, Zn and Sr together with the corresponding XRF images of the elements Ca, P, Sr, Zn, Fe, Cu detected. XRF shows three images of the leg for the elements Ca, K and Fe, acquired with the developed scanning device.

However when trying to map a chicken leg, as reported in Fig. 5, there is an increase in scattered photons due to the presence of the skin and meat before the bone, which decreases the peak-background ratio and implies the need to

improve the technique of data acquisition and analysis that enables the reduction of the fund.

This difficulty is also present in conventional techniques of *in-vivo* XRF and it may imply a significant increase in the calculated dose depending on the item and the place where XRF scanning is applied.

4. Conclusions

This work presented a complete dosimetric study devoted to characterize the developed *in-vivo* X-ray Fluorescence scanning device assessing the corresponding delivered dose levels when using it for routine applications in patients. Absorbed dose along with corresponding dose distributions have been calculated by means of simplified analytical model as well as full stochastic Monte Carlo simulations. Dose calculations have been performed for homogeneous (tissue-equivalent) and heterogeneous (bone-tissue) biological samples and the obtained results have shown an overall good agreement. In addition, the reported results are also in very good correspondence with data previously published by other authors.

The *in-vivo* XRF device by means of XRF scanning produces images in shorter time, which implies general reduction of the absorbed dose in comparison to conventional techniques.

Acknowledgements

This work has been supported by FONDECYT Project number 1080306 and grants from University of La Frontera, Chile.

1. V. Somerset, L. Petrik, R. White, M. Klink, D. Keyb and E. Iwuoha, *Talanta* **64** (2004) 109.
2. N. Jianjun, P. Rasmussen, A. Wheeler, R. Williams, and R. Chenier, *Atmospheric Environment* **44** (2010)235.
3. M. Sabel and H. Aichinger, *Physics in Medicine and Biology* **41** (1996) 315.
4. G. Tirao, C. Quintana, and M. Valente, *International Journal of Low Radiation* **7** (2010) 276.
5. F.A. Dilmanian, Z. Zhong, B. Ren, X.Y. Wu, L.D. Chapman, I. Orion, and W.C. Thomlinson, *Physics in Medicine and Biology* **45** (2000) 933.
6. T. Radu and D. Diamond, *Jour. of Hazardous Mat.* **171** (2009) 1168.
7. E. Marguá, I. Queralt, and M. Hidalgo, *Trends in Analytical Chemistry* **28** (2009) 362.
8. L. Vincze *et al.*, *Proceedings of the SPIE* **5535** (2004) 220.
9. M. Farquharson, K. Geraki, G. Falkenberg, R. Leek, and A. Harris, *Applied Radiation and Isotopes* **65** (2007) 183.
10. F. El-Amri and M. El-Kabroun, *Radioanal. Nucl. Chem.* **217** (1997) 205.
11. A. Gustafsson, B.K. Lind, and A. Brahme, *Med Phys.* **21** (1994) 343.
12. A. Eklöf, A. Ahnesjö, and A. Brhame, *Acta Oncol.* **29** (1990) 447.
13. F. Salvat, J.M. Fernandez-Varea, and J. Sempau, *PENELOPE-2008: A Code System for Monte Carlo Simulation of Electron and Photon Transport* (ISBN 978-92-64-99066-1) (No. 6416, France, 2008).
14. M. Valente, F. Malano, and G. Tirao, *International Journal of Low Radiation* **7** (2011)333
15. F. Botta *et al.*, *Jour. Nucl. Med.* **50** (2009) 1859.
16. G. Gambarini *et al.*, *Jour. Phys: Conf. Series* **4** (2006) 466.
17. G. Castellano D. Brusa, M. Carrara, G. Gambarini, and M. Valente, *Nucl. Instrum. Meth. A* **580** (2007) 502.